Dissolution Kinetics of Carboxylic Acids I: Effect of pH under Unbuffered Conditions

K. G. MOONEY *, M. A. MINTUN ‡, K. J. HIMMELSTEIN, and V. J. STELLA ×

Received March 24, 1980, from the *Departments of Pharmaceutical Chemistry and Chemical and Petroleum Engineering, University of Kansas, Lawrence, KS 66045.* Accepted for publication July 3, 1980. *Present address: Boehringer Ingelheim, Ridgefield, CT 06877. ‡Present address: Washington University, St. Louis, MO 63110.

Abstract □ The dissolution behavior of benzoic acid, 2-naphthoic acid, and indomethacin from rotating compressed disks into aqueous solutions of constant ionic strength (μ = 0.5 with potassium chloride) at 25° was investigated. The pH of the bulk aqueous medium was maintained during dissolution by means of a pH-stat apparatus. A model for the initial steady-state dissolution rate of a monoprotic carboxylic acid was derived from Fick's second law of diffusion. This model assumed that diffusion-controlled mass transport and simple, instantaneously established reaction equilibria existed across a postulated diffusion layer. Using previously determined intrinsic solubilities, pKa values, and diffusion coefficients, the model was found to predict the dissolution rates of these acids accurately as a function of the bulk solution pH. Hydroxide ion and water were the only reactive base species present in the bulk solution. The concentration profiles of all of the species across the diffusion layer were generated for a given bulk pH. Furthermore, the model generated values for the pH profile within the microclimate of the diffusion layer and the pH at the solid–solution boundary.

Keyphrases □ Dissolution kinetics—carboxylic acids, effect of pH under unbuffered conditions □ Carboxylic acids—dissolution kinetics, effect of pH under unbuffered conditions □ Kinetics—dissolution of carboxylic acids, effect of pH under unbuffered conditions

The purpose of this study was to examine the effect of solubility and unbuffered bulk solution pH on the dissolution kinetics of three carboxylic acids: benzoic acid (I), 2-naphthoic acid (II), and indomethacin (III). The dissolution of carboxylic acids into a basic medium represents dissolution with a simultaneous, instantaneous, reversible chemical reaction. Modeling of this system should allow determination of the solid–liquid interfacial pH and the composition of the diffusion layer (1), the unstirred liquid layer postulated to exist adjacent to the solid surface.

The dissolution kinetics of acidic compounds into a basic medium were studied initially by Brunner (2) and later by other investigators (3–7). Factors that affect the dissolution of benzoic acid, which undergoes a simultaneous chemical reaction with basic species from the bulk solution,

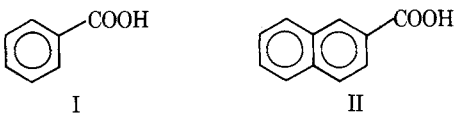

I

II

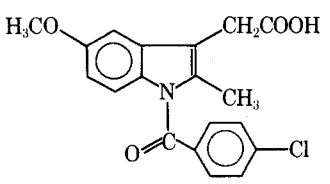

III

were studied and modeled in detail by Higuchi *et al.* (5). They used the film theory of Nernst (1), which is based on Fick's laws of diffusion (8).

To investigate the initial dissolution rates of I–III over a wide range of bulk pH values without using buffers, automatic potentiometric monitoring employing a pH-stat system can be employed (9–13). This technique, combined with a rotating-disk apparatus similar to that described by Wood *et al.* (14), results in a constant dissolution surface area. The hydrodynamic theory of Levich (15) was applied to rotating disks (16, 17). From this theory, the thickness of the diffusion layer may be calculated and used in a modified Nernst (1) expression to predict initial dissolution rates (16, 17).

A simplified equation was used to describe the dissolution of acids in a basic medium (18, 19). However, this equation is derived by assuming that the bulk solution pH and the interfacial pH, pH_0, are identical. However, the bulk hydrogen-ion concentration is not necessarily equal to that at the solid–liquid interface or elsewhere within the diffusion layer. The interfacial pH is affected by the degree of dissociation of the acid at the interface, which is determined by the concentration and pKa of the acid. Dissociation of the acid liberates hydrogen ions, thereby lowering the pH of the diffusion layer relative to that of the bulk solution.

THEORETICAL

The starting point for a model of dissolution of an acid in a basic medium comes from the work of Higuchi *et al.* (5). Their model was formulated around that of Nernst (1) for a diffusion-controlled process in the solution phase and postulates the existence of a diffusion layer (a region of unstirred solvent) adhering to the dissolving surface. Within this layer, all concentration gradients of reactants and products are postulated to exist as a result of diffusion and the chemical reaction between the dissolving solute and the incoming base from the bulk solution. The bulk solution is regarded as a homogeneous mixture with no concentration gradients.

Figure 1 is a pictorial representation of the model where a solid carboxylic acid, HA, dissolves at the phase boundary. At the solid–liquid interface, the boundary condition is $X = 0$ and the concentration of HA is $[HA]_0$, which is the saturated solubility of the unionized acid. The acid diffuses and simultaneously reacts with the incoming base (B^-) or water to give the conjugate base (A^-) and HB. The diffusion layer has a thickness h; the model specifies that, for the limit $X = h$, [HA] and $[A^-]$ are effectively zero under sink conditions.

The model also specifies that, at steady state, the acid–base reaction occurs anywhere within the diffusion layer and any equilibrium formed between the reacting species is regarded as being established instantaneously, *i.e.*, the diffusional processes are slow relative to the chemical

0022-3549/81/0100-0013$01.00/0

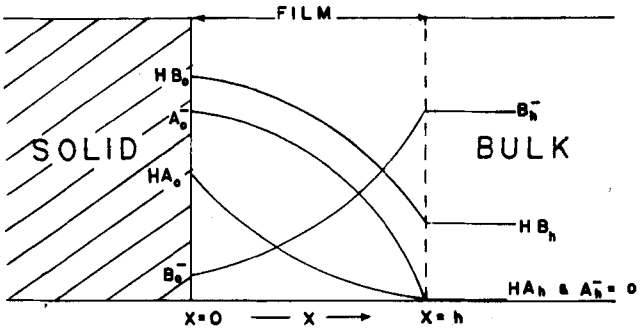

Figure 1—*Schematic diagram of the model of Higuchi* et al. *(5) for the dissolution of an acid, HA, into a reactive medium containing base, B^- (A^- and HB are products of the reaction).*

processes (reaction). Individual diffusivities for all components must be accounted for in the model.

The present model describes the dissolution of an acid in a system where the only reactive base species are hydroxide ion and water. The equilibria involved are given in Schemes I and II.

$$H_2O + HA \overset{K_a^*}{\rightleftharpoons} H_3O^+ + A^-$$

Scheme I

$$H_3O^+ + OH^- \rightleftharpoons 2\,H_2O$$

Scheme II

For simplicity, H_3O^+ may be regarded as hydrogen ion (H^+). When the equilibria are combined, they produce the situation shown in Scheme III, which also was used by Higuchi *et al.* (5).

$$HA + OH^- \overset{K_1^*}{\rightleftharpoons} H_2O + A^-$$

Scheme III

In the model of Higuchi *et al.* (5), only Scheme III was considered for the chemical reaction of HA with hydroxide ion. By including the equilibria of Schemes I and II, the general applicability of this model is broadened.

The equilibrium constants for Schemes I–III are given by:

$$K_a = \frac{[H^+][A^-]}{[HA]} \quad \text{(Eq. 1)}$$

$$K_w = [H^+][OH^-] \quad \text{(Eq. 2)}$$

$$K_1 = \frac{[A^-]}{[HA][OH^-]} \quad \text{(Eq. 3)}$$

where $[H_2O]$ is regarded as constant and is included in the relevant equilibrium constants and H_3O^+ is equivalent to H^+.

Application of Fick's Laws of Diffusion to Dissolution with Simultaneous Chemical Reaction—When a chemical reaction occurs between diffusing species, the mass balance of any species across the diffusion layer involves not only diffusion into and out of any element but also the chemical reaction, which simultaneously changes the effective concentrations of the species at any given point X. To account for the simultaneous chemical reaction, a reaction rate function, ϕ, is introduced into the steady-state equations for each species. At present, this function will remain undefined. At steady state and by utilizing Fick's laws of diffusion, the following equations can be written for all of the relevant species:

$$\frac{\partial[HA]}{\partial t} = D_{HA}\frac{\partial^2[HA]}{\partial X^2} + \phi_1 = 0 \quad \text{(Eq. 4)}$$

$$\frac{\partial[OH^-]}{\partial t} = D_{OH}\frac{\partial^2[OH^-]}{\partial X^2} + \phi_2 = 0 \quad \text{(Eq. 5)}$$

$$\frac{\partial[A^-]}{\partial t} = D_A\frac{\partial^2[A^-]}{\partial X^2} + \phi_3 = 0 \quad \text{(Eq. 6)}$$

$$\frac{\partial[H^+]}{\partial t} = D_H\frac{\partial^2[H^+]}{\partial X^2} + \phi_4 = 0 \quad \text{(Eq. 7)}$$

where $\phi_{1\text{-}4}$ are the reaction rate functions. Equations 4–7 are equal to zero under steady-state conditions. When a chemical reaction occurs in the diffusion layer between species, there is a finite rate of change of flux with X. Alternatively, the concentration profile of a species across the diffusion layer is not represented by a simple linear relationship, as in the Noyes–Whitney model, but instead by a curve whose rate of change of the slope at any point is dependent on the reaction of that species at that point.

Independently of Eqs. 4–7, relationships between rates of change of flux for the various species can be described by mass balance equations across the diffusion layer. Therefore, by mass balance:

$$D_{HA}\frac{d^2[HA]}{dX^2} = -D_A\frac{d^2[A^-]}{dX^2} \quad \text{(Eq. 8)}$$

and:

$$D_{OH}\frac{d^2[OH^-]}{dX^2} = D_{HA}\frac{d^2[HA]}{dX^2} + D_H\frac{d^2[H^+]}{dX^2} \quad \text{(Eq. 9)}$$

Equation 8 shows that any change in the HA flux due to a chemical reaction must mean that the flux of A^- changes in the opposite direction. Equation 9 states that OH^-, while diffusing in, will react with both HA and H^+ simultaneously as defined by the equilibrium constants in Schemes I and II. Hence, any change in the flux of OH^- must be reflected by corresponding changes in HA and H^+. Comparing Eqs. 8 and 9 to Schemes I and II and Eqs. 1–7 shows that:

$$\phi_1 = -\phi_3 \quad \text{(Eq. 10)}$$

or:

$$D_A\frac{d^2[A^-]}{dX^2} = \phi_1 \quad \text{(Eq. 11)}$$

and:

$$\phi_2 = \phi_1 + \phi_4 \quad \text{(Eq. 12)}$$

Integrating Eqs. 8 and 9 once gives:

$$D_{HA}\frac{d[HA]}{dX} = D_{OH}\frac{d[OH^-]}{dX} - D_H\frac{d[H^+]}{dX} + C_1 \quad \text{(Eq. 13)}$$

$$D_{HA}\frac{d[HA]}{dX} = -D_A\frac{d[A^-]}{dX} + C_2 \quad \text{(Eq. 14)}$$

where C_1 and C_2 are constants of integration. It can be shown that C_1 and C_2 are equal by mass balance considerations based on Schemes I and III. Substituting for C_2 in Eq. 14 and integrating with respect to X in Eqs. 13 and 14 give the following linear equations:

$$D_{HA}[HA] = D_{OH}[OH^-] - D_H[H^+] + C_1X + C_4 \quad \text{(Eq. 15)}$$

and:

$$D_{HA}[HA] = -D_A[A^-] + C_1X + C_3 \quad \text{(Eq. 16)}$$

where C_3 and C_4 are additional constants of integration.

Equations 15 and 16 must be given boundary conditions to allow evaluation of the resulting constants.

Boundary Conditions—

At $X = 0$:

$[HA]_0$ = solubility of HA
$[OH^-]_0$ = unknown
$[H^+]_0$ = unknown
$[A^-]_0$ = unknown

At $X = h$:

$[HA]_h$ = 0 (under sink conditions)
$[OH^-]_h$ = from bulk pH
$[H^+]_h$ = from bulk pH
$[A^-]_h$ = 0 (under sink conditions)

Evaluation of Constants and Conditions at $X = 0$—Utilizing these boundary conditions ($X = 0$ and $X = h$), Eqs. 15 and 16 and 2 and 3 at $X = 0$, and algebraically solving for $[H^+]_0$ yield:

$$-D_H[H^+]_0^2 + [H^+]_0(D_H[H^+]_h - D_{OH}[OH^-]_h) + K_w(D_{OH} + D_AK_1[HA]_0) = 0 \quad \text{(Eq. 17)}$$

Equation 17 is of the type:

$$az^2 + bz + c = 0 \quad \text{(Eq. 18)}$$

where:

$z = [H^+]_0$
$a = -D_H$
$b = D_H[H^+]_h - D_{OH}[OH^-]_h$

$$c = K_w(D_{OH} + D_A K_1[HA]_0)$$

the solution of which is:

$$z = \frac{-b \pm \sqrt{b^2 - 4ac}}{2a} \quad \text{(Eq. 19)}$$

By considering the possible signs of the coefficients a, b, and c in Eq. 19, it may be shown that only:

$$z = \frac{-b - \sqrt{b^2 - 4ac}}{2a} \quad \text{(Eq. 20)}$$

will be the correct root. Having obtained $[H^+]_0$, all of the other unknowns, including C_1–C_4, may be calculated in a sequential manner from the preceding equations since all of the constants required in the quadratic expression (Eq. 17) are known or can be estimated.

Expression for Total Flux of Acids at Any Given Bulk Solution pH—The concentrations of all species at the solid–liquid interface, *i.e.*, where $X = 0$, can be calculated. An expression for the total flux of the dissolving acid is now required as a function of changing conditions in the bulk solution or at $X = h$.

Again, from Eqs. 15 and 16 and the stated boundary conditions:

$$C_1 = -\left(\frac{D_{HA}[HA]_0}{h}\right) + \frac{D_H}{h}([H^+]_h - [H^+]_0) + \frac{D_{OH}}{h}([OH^-]_0 - [OH^-]_h) \quad \text{(Eq. 21)}$$

where the right side of Eq. 21 is exactly the negative of the total flux of species across the diffusion layer. Thus:

$$J^{total} = -C_1 = \frac{D_{HA}}{h}[HA]_0 + \frac{D_H}{h}([H^+]_0 - [H^+]_h) + \frac{D_{OH}}{h}([OH^-]_h - [OH^-]_0) \quad \text{(Eq. 22)}$$

and:

$$J^{total} = J_{HA} + J_H + J_{OH} = -C_1 \quad \text{(Eq. 23)}$$

where J^{total} is the total flux of HA from the solid surface at $X = 0$. Paradoxically, there is no expression relating the flux for the diffusion of A^- across the diffusion layer because the fluxes of H^+ and OH^- automatically account for that of A^-. Equation 22 differs from that derived by Higuchi *et al.* (5) in that it includes the terms for $[H^+]$, but it is similar to the equations of Hamlin and Higuchi (7) and Tsuji *et al.* (17).

It is important to examine some conditions where the different parts of Eq. 22 exert their influence on the total flux or dissolution rate from the solid surface.

1. The case where the bulk pH is considerably lower than the pKa of the dissolving acid, *i.e.*, $[H^+]_h \gg K_a$. Under this condition, the ionization of the acid is suppressed within the diffusion layer, making $[H^+]_0$ and $[H^+]_h$ (and, hence, $[OH^-]_0$ and $[OH^-]_h$) equal. The total flux then is given by:

$$J^{total} = \frac{D_{HA}[HA]_0}{h} \quad \text{(Eq. 24)}$$

for the case of sink conditions (*i.e.*, $[HA]_0 \gg [HA]_h$).

2. The case where the bulk solution pH is increased such that it no longer suppresses ionization in the film. Thus, HA is able to dissociate (due to interaction with water) as described by Scheme I and Eq. 1.

Hence, in pH regions around the pKa of the acid and up to neutrality in the bulk solution, the dominant form of the equation is:

$$J^{total} = \frac{D_{HA}[HA]_0}{h} + \frac{D_H}{h}([H^+]_0 - H^+]_h) \quad \text{(Eq. 25)}$$

The flux of OH^- will not be zero, but, in this region, it is negligible compared to the flux of HA and H^+.

3. The case where the bulk solution pH is increased such that $[OH^-]_h$ approaches $[HA]_0$. The controlling factor in dissolution now is the diffusion of hydroxide ion into the diffusion layer and the reaction with HA as given by the equilibrium described in Scheme III and Eq. 3.

Thus, as HA is diffusing across the diffusion layer, the reaction with water and hydroxide ion occurs simultaneously. Hence, the total flux now is given by the full expression described in Eq. 22.

Therefore, for an accurate description of the total flux of acid where water and hydroxide ion are the only reactants in the bulk solution, it is necessary to consider $[HA]_0$, the intrinsic solubility of the acid, K_a, the dissociation constant of the acid, and the diffusivities of the acid, hydrogen, and hydroxide ions.

The concentrations of all of the species may be determined at any point X in the diffusion layer to observe their concentration profiles. At any distance across the diffusion layer ($X = X$), Eqs. 2, 3, 15, and 16 apply. The unknowns [HA], $[A^-]$, $[OH^-]$, and $[H^+]$, without subscripts, represent the concentrations of the respective species at position X in the diffusion layer. The process of solving for a particular unknown is similar to that given in the previous section for the solution at $X = 0$, except that [HA] also is an unknown. The C_1, C_4, and C_3 values previously were numerically determined from bulk solution boundary conditions in solving for the concentration of a species at $X = 0$.

The concentration of any one species may be solved for, but $[H^+]$ will give better insight at any particular position in the film. Hence, using Eqs. 3 and 15 to convert $[OH^-]$ to terms in $[H^+]$:

$$D_{HA}[HA] = \frac{D_{OH}K_w}{[H^+]} - D_H[H^+] + C_1X + C_4 \quad \text{(Eq. 26)}$$

To express [HA] in terms of $[H^+]$, Eqs. 3 and 16 must be used:

$$D_{HA}[HA] = \frac{-D_A[HA]K_1K_w}{[H^+]} + C_1X + C_3 \quad \text{(Eq. 27)}$$

Collecting terms in Eq. 27:

$$[HA] = (C_1X + C_3)\left(\frac{[H^+]}{D_{HA}[H^+] + D_AK_1K_w}\right) \quad \text{(Eq. 28)}$$

Equation 28 now may be substituted into Eq. 26 to give:

$$D_{HA}(C_1X + C_3)\left(\frac{[H^+]}{D_{HA}[H^+] + D_AK_1K_w}\right) = \frac{D_{OH}K_w}{[H^+]} - D_H[H^+] + C_1X + C_4 \quad \text{(Eq. 29)}$$

Multiplying Eq. 29 by $[H^+]$ $(D_{HA}[H^+] + D_AK_1K_w)$ and collecting terms give:

$$p[H^+]^3 + q[H^+]^2 + r[H^+] + s = 0 \quad \text{(Eq. 30)}$$

where:

$$p = -D_AD_{HA}$$
$$q = C_4D_{HA} - C_3D_{HA} - D_AK_1K_wD_H$$
$$r = K_w(D_{HA}D_{OH} + C_4D_AK_1 + C_1XD_AK_1)$$
$$s = D_AD_{OH}K_1K_w^2$$

The form of Eq. 30 is cubic, with the relevant coefficients being represented as p, q, r, and s as defined. As such, Eq. 30 has three roots for $[H^+]$. The correct solution was found by the iterative method of Newton (20) utilizing a digital computer[1].

Once $[H^+]$ is calculated from Eq. 30, sequential solution of Eqs. 15, 16, 2, and 3 enables $[OH^-]$, [HA], and $[A^-]$ to be determined and the diffusion layer profiles for all species to be calculated.

Calculation of Film Thickness (h)—The Levich rotating-disk model provides a technique for following the dissolution of a solid drug from a compressed disk that maintains a constant surface area during dissolution. The Levich (15) model defines the film thickness as:

$$h = 1.612D^{1/3}\nu^{1/6}\omega^{-1/2} \quad \text{(Eq. 31)}$$

where D is the diffusivity, ν is the kinematic viscosity of the medium, and ω is the angular velocity in radians per unit time.

The Levich theory used here is based on a single diffusing species with the boundary layer thickness dependent on the diffusion coefficient of that species to the one-third power (15). In the current study, there are several diffusing species with different transport properties; thus, the assumption of a constant-thickness boundary layer may not be correct where the diffusivity of a possible reaction- and flux-controlling species, *e.g.*, hydroxide ion, is significantly different from that of the acid, HA. As will be seen later, the total flux equation (Eq. 22) can collapse to where the diffusivity of hydroxide ion becomes a dominant term. Thus, the error contribution to the calculated fluxes could occur only at high pH. However, the differences in the calculated boundary layer thickness considering the differences in the diffusivities are dampened by the one-third power dependency of the thickness on diffusivity. Although it may be possible to derive a theoretical extension of the Levich approach for a multispecies system, it will be assumed that the simplified theory of a single-thickness layer presented here is reasonable considering the scope and intent of this work.

The Noyes–Whitney or Nernst–Brünner model describes the flux (J)

[1] Honeywell model 66/60. A copy of the procedure and program can be obtained from V. J. Stella.

of the acid under sink conditions, where no chemical reactions occur, as $J = D_{HA}C_s/h$, where C_s is $[HA]_0$.

By combining this equation and Eq. 31, the following expression is obtained:

$$J = 0.62D_{HA}^{2/3}\nu^{-1/6}C_s\omega^{1/2} \quad \text{(Eq. 32)}$$

where J is proportional to the square root of the rotation speed.

EXPERIMENTAL

Materials—Benzoic acid[2], 2-naphthoic acid[3], and indomethacin[4] were obtained in the pure, crystalline form. Benzoic acid was used as supplied, while 2-naphthoic acid was recrystallized from 95% ethanol according to the method of Perrin *et al.* (21). Indomethacin, despite high purity, was not in a suitable form for disk formation under high compression. Using a method described by Pakula *et al.* (22), the α-form of indomethacin was prepared, which is the lowest melting form of the compound but has been shown by Pakula *et al.* (23) to be stable.

All other chemicals were reagent grade and were not purified further.

Solubility and pKa Determinations—The intrinsic solubility (*i.e.*, the solubility of the undissociated species) of a monoprotic weak acid and its corresponding pKa may be determined simultaneously by measuring the total solubility of the acid as a function of pH under controlled ionic strength and temperature conditions. This method was described previously (24, 25) and is readily applied to compounds of poor aqueous solubility. This solubility method was used to determine the solubilities and pKa values of the acids at an ionic strength of 0.5 (with potassium chloride) and 25 ± 0.5° in a range of hydrochloric acid or 0.1 *M* acetate buffers.

Excess solid acid was shaken for at least 48 hr in vials containing ~10 ml of buffer at 25 ± 0.5° in a shaking water bath[5]. In all cases, 48 hr was sufficient for obtaining equilibrium solubility. Indomethacin is subject to decomposition by light and hydrolysis (26–28) in aqueous solutions. By excluding light from the vials and optimizing the equilibration time, these problems were shown to be insignificant. It was approximated from data given by previous investigators that the half-life for hydrolysis in the pH region of interest (pH 2–5) was considerably longer than the time required for equilibration during the solubility studies.

After equilibration, the solutions were filtered using a 5.0-μm membrane filter[6], and portions of the filtrate were diluted appropriately with 0.1 *M* HCl. Concentrations of all compounds were measured using a UV–visible spectrophotometer[7] with the appropriately diluted buffer solution as the reference. The wavelengths and molar absorptivity for measurement of the three acids are given in Table I. The pH of the filtrate prior to detection was measured at 25° using a combination microelectrode[8] and a pH meter[8]. All samples were run at least in duplicate.

Determination of Dissolution Rates—The procedure for following the initial dissolution rates of the three acids was similar to that of Tsuji *et al.* (17) and Underwood and Cadwallader (13). The apparatus (Fig. 2) was based on the rotating-disk method of Nogami *et al.* (29) and Wood *et al.* (14). It consisted of three main parts: the dissolution cell and rotating disk, the pH-stat with a measuring electrode, and the detection system for continuous monitoring of the bulk solution concentration in the dissolution cell.

The dissolution cell consisted of a water-jacketed beaker maintained at 25 ± 0.1°[9]. The dissolution medium (250 ml) was placed in the cell into which was immersed a combination pH electrode, a Plexiglas disk holder[10] with a shaft, and a titrant delivery tube. Also, two sampling tubes, which were connected to a flowthrough system, were placed in the solution at set positions to sample and return the solution during a dissolution run.

The shaft and disk holder were rotated by an overhead synchronous motor of variable speed[11] that was calibrated by a tachometer[12]. Disks of solid material, previously compressed to a precise size, were inserted into the holder to form a surface flush with that of the disk holder. The

Table I—Spectral Characteristics of the Three Carboxylic Acids Used in Solubility Studies (25°)

Compound	λ_{max}, nm	ϵ_{molar}	Solvent for Measurement
Benzoic acid	229	11,375	0.01 *M* HCl
2-Naphthoic acid	235	54,332	0.01 *M* HCl
Indomethacin	264	17,926	0.01 *M* HCl or 0.1 *M* acetate buffer

pH electrode and titrant tubing were connected to the pH-stat assembly, which continuously monitored the pH of the medium during a dissolution run and delivered titrant to maintain a predetermined pH within that medium. Once steady-state conditions were reached during a dissolution run, the titrant was delivered at a constant rate, which was dependent on the release rate of acid from the disk and the concentration of titrant used. In all cases, sodium hydroxide solution was the titrant and ranged from 0.01 to 0.5 *M*, depending on the acid and the pH being maintained.

The continuous monitoring device was a flow system with a UV spectrophotometer[13]. The spectrophotometer, equipped with a flowcell with a 1-cm path length, was set to measure the acid concentration in the bulk solution at the optimum wavelength of absorbance for each compound after standardization. A peristaltic pump[14] circulated the solution using silicon tubing of fine bore (4.1 mm o.d. × 0.76 mm i.d.); the remainder of the tubing was made of polytef[15] (1.5 mm o.d. × 0.8 mm i.d.) to reduce potential adsorption during an experiment.

When dissolution experiments were performed under acidic conditions (*i.e.*, pH 2.00), the pH-stat system was not required due to the suppression of any ionization of the dissolving acid. However, to maintain consistent hydrodynamics between runs performed at varying pH, the pH electrode and delivery tubing were not removed. To determine if the compounds dissolved by a diffusion-controlled mechanism, the dissolution rates of the acids were measured (where possible) at pH 2.00 over a range of rotation speeds.

Disk Preparation—Individual disks of 200–500 mg of each compound were compressed at 4.5×10^3 kg for 1 min using an IR potassium bromide pellet punch and die[16] in a hydraulic press[17]. The disks were 1.3 cm in diameter and of varying thickness, depending on the amount and compressibility of the material used. Benzoic acid and 2-naphthoic acid were compressed directly, but indomethacin presented some difficulty due to capping. The γ-polymorph of indomethacin (mp 160–162°) was the

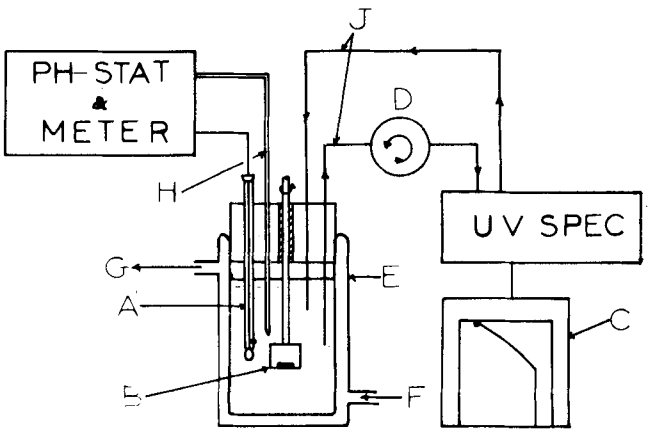

Figure 2—*Diagram of the rotating disk and cell, the pH-stat and concentration monitoring devices, the combination electrode (A), the Plexiglas disk holder with disk (B), the recorder for concentration* versus *time readout (C), the peristaltic pump (D), the thermostated-jacketed dissolution cell (E), the water jacket inlet (F), the water jacket outlet (G), the delivery tubing from the pH-stat (H), and the circulating tubing for the UV flowcell (J).*

[2] Fisher Scientific Co., Fair Lawn, N.J.
[3] Aldrich Chemical Co., Milwaukee, Wis.
[4] Merck Sharp & Dohme, West Point, Pa.
[5] American Optical Corp., Buffalo, N.Y.
[6] Gellman Metrical, 13 mm.
[7] Cary Instruments model 118.
[8] Radiometer Instruments, Copenhagen, Denmark.
[9] Model Fe Haake Instruments, Karlsruhe, West Germany.
[10] Manufactured at the University of Kansas.
[11] Model T2, G. K. Heller Corp., Floral Park, Long Island, N.Y.
[12] Tak-ette, Power Instruments, Skokie, Ill.
[13] Carl Zeiss, New York, N.Y.
[14] Masterflex, Cole-Parmer, Chicago, Ill.
[15] Rainin Instrument Co., Brighton, Mass.
[16] Coleman Products, England.
[17] Carver Press, Fred Carver, N.J.

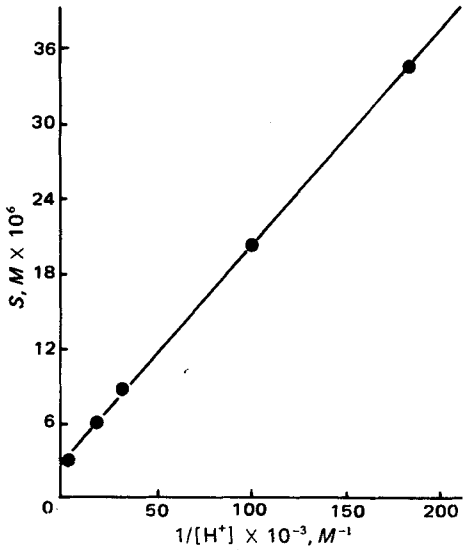

Figure 3—*Plot of total solubility of indomethacin at 25° versus 1/[H⁺] for equilibrated 0.1 M acetate buffers, μ = 0.5 (potassium chloride); S_0 is obtained from the intercept, and K_a is obtained from the slope.*

worst for disk formation, while the α-form was suitable.

According to IR measurements (23) before and after compression, no appreciable amount of γ-indomethacin was formed during compression so the disks were regarded as being of uniform α-indomethacin. Where disk formation was hindered by capping and sticking, the material was compressed once, ground, and recompressed. Again, no apparent polymorphic changes were observed in the slugged α-indomethacin. It was assumed that the surface area of the disk did not change during dissolution, even though some pitting was seen with the more soluble compounds.

The rotation speed of the mounted disk was varied from 50 to 900 rpm, which corresponds to Reynolds numbers of 226–3983 as defined by:

$$Re = \frac{r^2\omega}{\nu} \qquad \text{(Eq. 33)}$$

where Re is the dimensionless Reynolds number and r is the radius of the disk. The Reynolds number range calculated here is well below that quoted by Levich (15) for transition from laminar to turbulent flow at the disk surface.

RESULTS AND DISCUSSION

Solubility and pKa—The total solubility of a monoprotic weak acid in aqueous solution is equal to the sum of the concentrations of the species appearing in solution at equilibrium, *i.e.*:

$$S = [HA]_0 + [A^-] \qquad \text{(Eq. 34)}$$

where S represents the total solubility and $[HA]_0$ and $[A^-]$ are as defined previously. Combining Eq. 34 with the K_a expression for the acid yields:

$$S = [HA]_0 + \frac{K_a[HA]_0}{[H^+]} \qquad \text{(Eq. 35)}$$

where $[H^+]$ is the hydrogen-ion concentration at equilibrium. A plot of

Table II—Measured Intrinsic Solubilities and K_a Values for Benzoic Acid, 2-Naphthoic Acid, and Indomethacin at 25° (±0.5°) and an Ionic Strength of 0.5 with Potassium Chloride

Compound	Intrinsic Solubility (HA_0), M	K_a	pKa	r^a
Benzoic acid	2.16×10^{-2}	9.25×10^{-5}	4.03	0.9999
2-Naphthoic acid	1.3×10^{-4}	9.64×10^{-5}	4.02	0.9998
Indomethacin	2.62×10^{-6}	6.70×10^{-5}	4.17	0.9996

[a] Correlation coefficient from plots of S *versus* $1/[H^+]$ (Eq. 35).

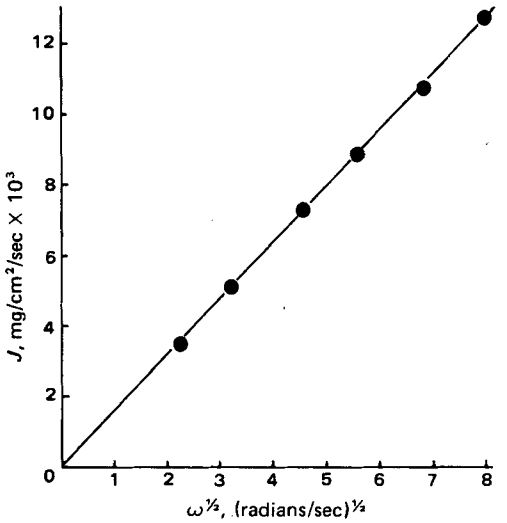

Figure 4—*Plot of the flux, J, of benzoic acid as a function of the square root of the rotation speed, ω, in 0.01 N HCl, μ = 0.5 (potassium chloride) at 25°.*

S versus $1/[H^+]$ yields an intercept of $[HA]_0$ and a slope of $K_a[HA]_0$. Dividing the intercept into the slope gives K_a. Figure 3 is such a plot for indomethacin. Similar plots were obtained for the other two acids, and the results are summarized in Table II.

Dissolution Rate as Function of Rotation Speed—The adherence to the Levich model for the dissolution of benzoic acid, 2-naphthoic acid, and indomethacin was examined. It was studied at a bulk solution pH of 2.00 for benzoic and 2-naphthoic acids. Indomethacin was too insoluble at this pH to give an accurate initial dissolution rate, especially at the lower rotation speeds. Hence, its dissolution rate study was carried out at pH 7.00.

It was assumed that the hydrodynamics at pH 7.00 were similar to those at pH 2.00. At the highest rotation speeds, an estimate of the initial dissolution rate of indomethacin was made at bulk pH 2.00. Indomethacin dissolution rates at pH 7.00, as a function of rotation speeds, were de-

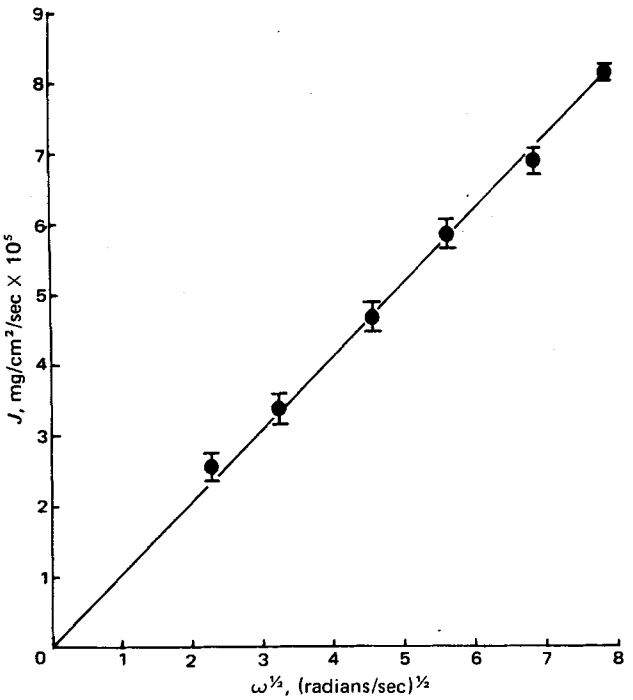

Figure 5—*Plot of the flux, J, of 2-naphthoic acid as a function of the square root of the rotation speed, ω, in 0.01 N HCl, μ = 0.5 (potassium chloride) at 25°. The error bars represent the standard deviation for each point.*

Table III—Data Obtained from Plots of J *versus* $\omega^{1/2}$ for Benzoic Acid, 2-Naphthoic Acid, and Indomethacin

Compound	Slope (Levich Plots)[a]	Calculated Diffusivity from Slope, cm²/sec	r^b
Benzoic acid	1.594×10^{-3}	9.6×10^{-6} [c]	0.9996
2-Naphthoic acid	1.003×10^{-5}	6.1×10^{-6} [c]	0.9986
Indomethacin	4.889×10^{-6}	5.0×10^{-6} [c,d]	0.9613

[a] Slope = $0.62D^{2/3}\nu^{-1/6}C_s$ from Eq. 36. [b] Correlation coefficient for least-squares linear plot of J *versus* $\omega^{1/2}$. [c] Using $\nu = 9.77 \times 10^{-3}$ Stokes from Ref. 31. [d] Surface pH calculated from Eq. 20.

termined with the pH-stat to maintain the bulk solution pH. It was assumed that a change in the rotation speed did not affect the mixing of the added base during dissolution. The results of the dissolution rates *versus* $\omega^{1/2}$ are given for each compound in Figs. 4–6. A summary of the slopes and diffusivities is given in Table III.

The linearity, intercepts, and slopes obtained in Figs. 4 and 5 suggest that a truly diffusion-controlled mechanism operates in the dissolution of benzoic and 2-naphthoic acids under acidic bulk pH. However, the indomethacin data do not agree with the theory in view of the pronounced nonzero intercept. The results suggest that dissolution occurs when the disk is static. The Levich theory considers only a forced-convection component due to rotation and ignores other mechanisms, such as natural convection, which may occur at low rotation speeds.

There are several possible reasons for the nonzero intercept with indomethacin. One is that the intrinsic error in the curve is large, as noted by the large standard deviations at each point, because the initial dissolution rates of indomethacin are slow and subject to greater errors than are those of the other two acids. Another possible cause is that the pH of the solution may influence the kinetics such that, with a compound as sensitive to changes in the bulk conditions as indomethacin, an additional mechanism at the surface may influence the dissolution. The possible source of this pH effect could be the assumption that the boundary layer thickness is dependent only on the diffusivity of the acid (HA) and not on the diffusivities of hydrogen and hydroxide ion, whose effects may be rotation rate dependent (see *Theoretical*). The source of an additional mechanism is unclear and was not investigated in the present study.

Theoretical and Observed Diffusion Coefficients—Tsuji *et al.* (17) found good agreement between diffusion coefficients derived from the Levich analysis of the dissolution rate and those determined by the diffusion cell method of Goldberg and Higuchi (30). Diffusion cell measurements were not performed for benzoic acid, 2-naphthoic acid, and indomethacin in the present study; literature values were used instead. Diffusion coefficients determined under identical conditions to those used here (25° at $\mu = 0.5$ with potassium chloride) are not found in the literature, but approximations are given in Table IV.

Flynn *et al.* (31) reviewed various ways of calculating diffusion coefficients in liquid and gaseous systems. The most commonly accepted way is to use the Stokes–Einstein equation which predicts that D is proportional to $M^{-1/3}$, where M is the molecular weight of the diffusing molecule.

Dayal *et al.* (34) showed that there is a good correlation between diffusivity and molecular weight to the negative one-half power of many organic compounds of pharmaceutical interest. This square root relationship would be consistent with drug molecules being planar rather than spherical.

To calculate the diffusivity from the Levich plot (Fig. 6) for indomethacin, the total concentration of ionized and unionized acid must be

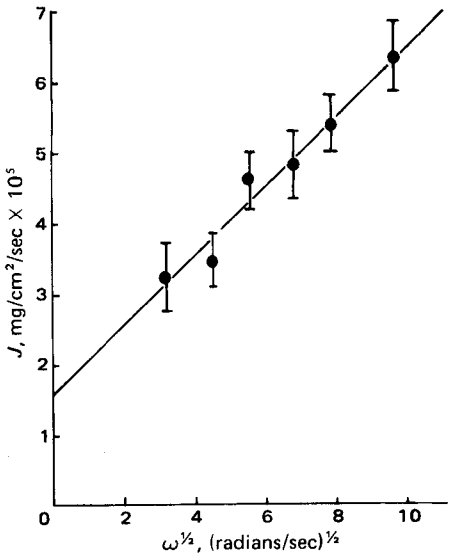

Figure 6—*Plot of the flux, J, of indomethacin as a function of the square root of the rotation speed, ω, in 0.5 M KCl, adjusted and maintained at pH 7.00 by a pH-stat at 25°. Error bars represent the standard deviation for each point.*

known at $X = 0$. By assuming a value of D_A in Eq. 17 and also the diffusivities of H^+ and OH^-, $[H^+]_0$ for bulk pH 7.00 may be calculated. A value of 5.6×10^{-6} cm²/sec for D_{HA} was calculated from the square root relationship, using benzoic acid as the reference. Having calculated $[H^+]_0$, the total indomethacin concentration at $X = 0$ can be obtained using Eq. 35. On substitution of this value for C_s into the Levich equation slope obtained from Fig. 6:

$$\text{slope} = 0.62D^{2/3}\nu^{-1/6}C_s \qquad \text{(Eq. 36)}$$

a value for the slope of 4.88×10^{-6} is calculated. Hence, good agreement is shown between the experimental and calculated values for the slope if a D_A value of 5.6×10^{-6} cm²/sec is assumed. This substitution also was tried using the Stokes–Einstein equation as a means of estimating the indomethacin diffusivity, but it failed to give a set of values as close as those from the square root relationship. Due to the presence of swamping electrolyte in the dissolution medium (0.5 M KCl) in all further calculations, the diffusivities of the conjugate bases of the acids are assumed to be equal to those of the acids.

Hydrogen and hydroxide-ion diffusivities have been discussed in the literature (32, 35–38). Many determinations have been performed using conductivity to obtain the diffusivities of the ions. However, according to Erdey-Grùz (37), care must be exercised in using diffusivity values from these sources since diffusional forces exerted on an ion in an electric field or across a potential gradient may not be identical to those in a neutral medium.

Stokes (35) determined the diffusivity of hydrochloric acid using a porous frit method and conditions similar to those employed here. He found a value of $D_H = 3.1 \times 10^{-5}$ cm²/sec at 25°, which is very close to the diffusivity of the hydroxide ion found by Higuchi *et al.* (5) in 0.75 M NaCl at 25°, $D_{OH} = 2.92 \times 10^{-5}$ cm²/sec. In the present study, it will be assumed that hydrogen and hydroxide ions have equal diffusivities (ignoring the effects of dissimilar hydration and ionic geometry in solution) which approximate the value for the self-diffusion of water. The value

Table IV—Diffusivity Data Available for Benzoic Acid, 2-Naphthoic Acid, and Indomethacin

Compound	Molecular Weight	D_{exp}[a] (25°, $\mu = 0.5$) cm²/sec	D_{theory} (Stokes–Einstein), cm²/sec	D_{theory}[b], cm²/sec	$D_{literature}$, cm²/sec
Benzoic acid	122.1	9.6×10^{-6}	6.63×10^{-6} [c]	8.90×10^{-6} [d]	11.0×10^{-6} [e] 12.1×10^{-6} [e]
2-Naphthoic acid	172.2	6.1×10^{-6}	6.11×10^{-6} [f]	8.08×10^{-6} [g]	—
Indomethacin	357.8	5.6×10^{-6} [g]	4.80×10^{-6} [h]	5.60×10^{-6} [g]	—

[a] From Figs. 4–6. [b] Using the square root relationship. [c] Using $\rho = 1.266$ g/ml, $T = 298$°K, and $\eta = 9.97 \times 10^{-3}$ poise. [d] Using *o*-aminobenzoic acid as the reference ($D = 8.4 \times 10^{-6}$ cm²/sec) at 25° in water from Ref. 33. [e] In water at 25° ($\mu = 0$) from Refs. 5 and 22. [f] Using $\rho = 1.40$ g/ml (T and η as for benzoic acid). [g] Using benzoic acid as a comparison. [h] Using 2-naphthoic acid as a comparison.

Table V—Initial Dissolution Rate Data for Benzoic Acid in 0.5 *M* KCl (μ = 0.5) with Varying Bulk Phase pH [a]

pH_{bulk}	pH_0 [b] (X = 0)	J_{obs}, moles/cm²/sec × 10^8 ($\pm SD$)	J_{theor} [c], moles/cm²/sec × 10^8
2.00	2.00	9.39 (±0.30)	9.06
3.00	2.83	—	9.55
4.00	3.05	—	9.93
5.00	3.08	—	9.98
6.00	3.08	—	9.99
7.00	3.08	9.60 [d]	9.99
8.00	3.08	9.16 (±0.43)	9.99
9.00	3.08	9.91 (±0.56)	9.99
10.00	3.11	9.50 (±0.33)	10.05
11.00	3.33	10.73 (±0.43)	10.08
11.20	3.45	11.14 (±0.10)	11.33
11.40	3.60	12.17 (±0.39)	12.33
11.70	3.87	14.58 (±0.43)	15.22
12.00	4.16	23.23 (±1.12)	21.19
12.30	4.46	33.53 (±3.10)	33.21
12.61	4.77	64.38 (±5.20)	58.38
13.04	5.20	136.31 [d]	141.89

[a] Rotation speed of the disk was 450 rpm for all dissolution rate measurements ($h = 2.31 \times 10^{-3}$ cm). [b] Calculated from Eq. 20. [c] Calculated from Eq. 22. [d] Mean taken from at least two determinations.

Table VII—Initial Dissolution Rate Data for Indomethacin in 0.5 *M* KCl (μ = 0.5) with Varying Bulk Phase pH [a]

pH_{bulk}	pH_0 [b] (X = 0)	J_{obs}, moles/cm²/sec × 10^{12} ($\pm SD$) [c]	J_{theor} [d], moles/cm²/sec × 10^{12}
2.00	2.00	12.17 (±3.0)	8.82
2.50	2.50	—	8.94
2.65	2.65	—	9.02
3.00	3.00	26.98 (±1.9)	9.34
3.50	3.50	—	10.61
4.00	4.00	30.99 (±3.38)	14.60
4.50	4.49	—	26.70
5.00	4.89	80.60 (±9.6)	54.80
6.00	5.19	133.59 (±12.9)	100.06
7.00	5.23	150.63 (±11.5)	108.02
7.50	5.24	166.00 (±2.7)	110.44
8.00	5.26	181.38 (±10.2)	116.68
8.50	5.34	227.21 (±8.3)	138.04
8.70	5.41	253.23 (±23.8)	158.32
9.00	5.56	338.16 (±9.3)	222.75
9.20	5.71	—	307.85
9.50	5.97	—	557.83

[a] Rotation speed of the disk was 600 rpm for all dissolution rate measurements ($h = 1.67 \times 10^{-3}$ cm). [b] Calculated from Eq. 20. [c] Standard deviation from at least three determinations. [d] Calculated from Eq. 22 and h calculated from Eq. 31.

assigned to the diffusivity of hydrogen ion and hydroxide ion was $D_H = D_{OH} = 2.80 \times 10^{-5}$ cm²/sec.

Initial Dissolution Rates as a Function of Bulk Solution pH—The initial dissolution rates of benzoic acid, 2-naphthoic acid, and indomethacin are given in Tables V–VII. These tables include the predicted or theoretical dissolution rates based on Eq. 22. To calculate these theoretical dissolution rates for given values of $[H^+]_h$ and $[OH^-]_h$, diffusion coefficients, $[HA]_0$ values, and equilibrium constants are used as previously determined or calculated. For comparative purposes, the relative dissolution ratio, R, is used, which normalizes the dissolution rates of all of the acids to the rate at pH 2.00, where the undissociated species is the only diffusant; R is defined by:

$$R = \frac{J}{J_0} = \left[\frac{D_{HA}[HA]_0 - D_H([H^+]_0 - [H^+]_h) + D_{OH}([OH^-]_h - [OH^-]_0)}{D_{HA}[HA]_0}\right] \quad \text{(Eq. 37)}$$

Both R_{theor} (theoretical) and R_{obs} (experimental) values are plotted *versus* bulk solution pH in Fig. 7. It can be seen from Eq. 37 that R is independent of h, the diffusion layer thickness. Hence, benzoic acid and 2-naphthoic acid data obtained at 450 rpm can be compared directly to the indomethacin data obtained at 600 rpm. For the calculation of the theoretical dissolution rates, h, as defined by the Levich relationship, was used for each compound at its designated rotation velocity as given by Eq. 31.

Tables V–VII indicate that, in all cases, there is reasonable agreement between the theoretical and predicted quantities, J_{theor}, and those obtained by experiment, J_{obs}. The theoretical values are based entirely on equations derived previously. Only independently determined or estimated parameters (*i.e.*, D_{HA} and $[HA]_0$) are used in these equations and no curve fitting actually was done.

The poorer agreement between J_{theor} and J_{obs} (Table VII) relative to R_{theor} and R_{obs} (Fig. 7) for indomethacin suggests that the value for either D_{HA} or $[HA]_0$ may be off. That is, if the solubility or diffusivity of indomethacin is underestimated by ~30%, it would account for the differences noted.

Figure 8 is a plot of the pH at the solid–liquid interface, pH_0, calculated

Table VI—Initial Dissolution Rate Data for 2-Naphthoic Acid in 0.5 *M* KCl (μ = 0.5) with Varying Bulk Phase pH [a]

pH_{bulk}	pH_0 [b] (X = 0)	J_{obs}, moles/cm²/sec × 10^{10} ($\pm SD$) [c]	J_{theor} [d], moles/cm²/sec × 10^{10}
2.00	2.00	4.28 (±0.18)	4.02
2.50	2.50	4.75 (±0.01)	4.10
2.65	2.65	4.91 (±0.25)	4.15
3.00	3.00	4.94 (±0.13)	4.36
3.50	3.49	5.85 (±0.17)	5.16
4.00	3.91	7.84 (±0.34)	7.11
4.50	4.15	10.28 (±0.64)	9.42
5.00	4.24	11.85 (±0.15)	10.64
6.00	4.28	13.30 (±0.40)	11.24
7.00	4.28	13.82 (±0.61)	11.31
8.00	4.29	13.59 (±0.43)	11.38
8.50	4.29	14.17 (±0.97)	11.63
9.00	4.32	14.99 (±0.24)	12.04
9.20	4.35	16.15 (±0.56)	12.50
9.50	4.41	18.24 (±1.07)	13.85
10.05	4.69	27.36 (±0.70)	22.58
10.20	4.80	34.62 (±1.45)	28.37
10.50	5.07	56.22 (±0.92)	49.43
10.70	5.27	—	74.90
11.00	5.56	—	144.36

[a] Rotation speed of the disk was 450 rpm for all dissolution rate measurements ($h = 1.99 \times 10^{-3}$ cm). [b] Calculated from Eq. 20. [c] Standard deviation from at least three determinations. [d] Calculated from Eq. 22 and h calculated from Eq. 31.

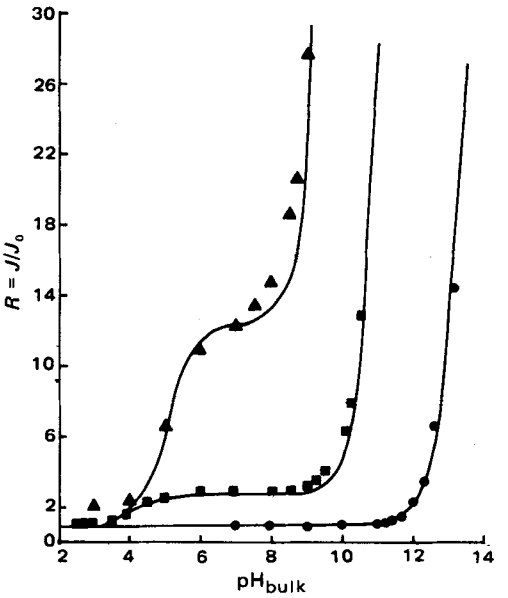

Figure 7—*Relative dissolution rate,* R, versus pH_{bulk} *for several carboxylic acids at 25°,* μ *= 0.5 (potassium chloride) using a pH-stat to maintain constant* pH_{bulk}. *The solid lines are those predicted by Eq. 22, and the data points are those experimentally determined;* J_0 *refers to the dissolution rate at pH 2.00,* μ *= 0.5. Key:* ▲, *indomethacin;* ■, *2-naphthoic acid; and* ●, *benzoic acid.*

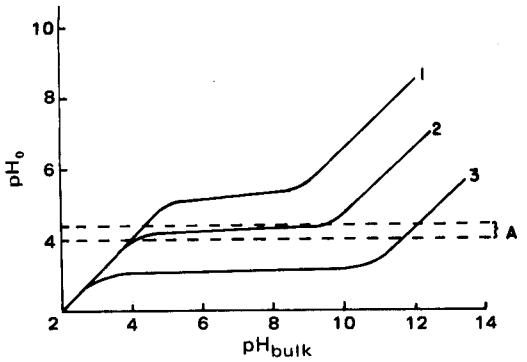

Figure 8—*Plot showing the relationship between the calculated pH at X = 0, pH_0, and pH_{bulk} for the dissolution of several carboxylic acids, where water and hydroxide ion are the only bases in the dissolution medium. Key: 1, indomethacin; 2, 2-naphthoic acid; and 3, benzoic acid.*

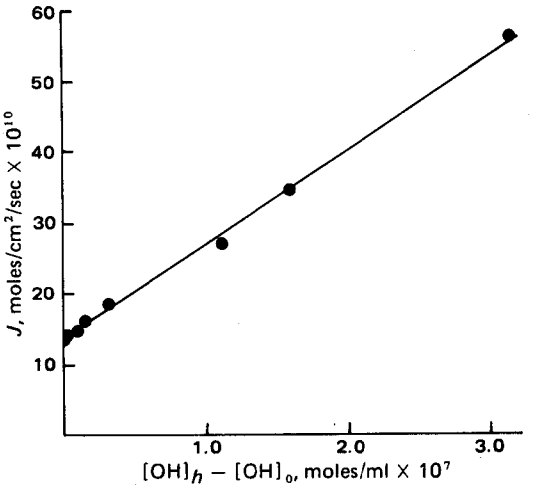

Figure 9—*Plot of the total dissolution rate of 2-naphthoic acid, J, as a function of the hydroxide-ion concentration difference across the diffusion layer of a rotating disk at 450 rpm.*

from Eq. 20 as a function of the bulk solution pH, pH_{bulk}, for each compound. In all cases, there are three clearly defined regions, which can be explained in terms of Eq. 22. The only parameters that differ between the compounds are the diffusivity (D_{HA} and D_A) and the intrinsic solubility ($[HA]_0$), assuming that the K_a values at $\mu = 0.5$ are approximately equal.

At very acidic bulk solution pH values, the pH at the solid–liquid interface equals that of the bulk because the hydrogen-ion concentration in the bulk solution is sufficient to suppress dissociation of the dissolving acids in the diffusion layer. Hence, the total concentration of the acid species at the solid–liquid interface is determined by the bulk solution pH or hydrogen-ion concentration and is the intrinsic solubility of the acid. Under these conditions, Nernst conditions exist since pH_0 equals pH_{bulk}. At lower bulk hydrogen-ion concentrations (larger pH_{bulk}), the acid dissociates to its conjugate base and hydrogen ions. This provides a larger total acid species concentration at $X = 0$, but hydrogen ions still limit the degree and amount of dissociation. As the bulk pH is increased or as $[H^+]_h$ decreases, benzoic acid, which is the most soluble of the acids studied, contributes to its own diffusion layer pH microenvironment at $X = 0$:

$$K_a[HA]_0 = [H^+]_0[A^-]_0 = [H^+]_0^2 \qquad \text{(Eq. 38)}$$

Alternatively, benzoic acid can be said to self-buffer the pH microenvironment of its diffusion layer. In Fig. 8, this is represented as a plateau between pH_{bulk} of ~3.0 and 11.0. In this region, pH_0 changes very little and remains at the pH value of ~3.08. This value would be the approximate pH of a saturated benzoic acid solution in 0.5 *M* KCl at 25°. In this region, the flux expression, Eq. 22, may be approximated by:

$$J = \frac{1}{h}(D_{HA}[HA]_0 + D_H[H^+]_0) \qquad \text{(Eq. 39)}$$

Since benzoic acid self-buffers at pH ~3.0, the increase in the total benzoate species concentration at $X = 0$ over a wide range of bulk pH is only ~10% of that at bulk pH 2.00, where ionization is essentially suppressed. Therefore, the relative dissolution rate for benzoic acid changes very little in this region. 2-Naphthoic acid and indomethacin, being less soluble than benzoic acid by factors of ~10^2 and 10^4, respectively, are less able to control or self-buffer the diffusion layer pH microenvironment at $X = 0$. Hence, lower hydrogen-ion concentrations in the bulk solution are required than for benzoic acid for the deviation from Nernst behavior to be observed. This change occurs at a pH_{bulk} of ~4.30 for 2-naphthoic acid and at a pH_{bulk} of ~5.20 for indomethacin. These pH values correspond again to those of saturated solutions of the two acids in 0.5 *M* KCl at 25°.

The plateau pH_0 values of 2-naphthoic acid and indomethacin correspond to 2.65 and 11.35 times, respectively, the total acid species concentration at $X = 0$ as there are at pH_{bulk} 2.00. Hence, the dissolution rates of 2-naphthoic acid and indomethacin are much more sensitive to changes in the bulk solution pH. This stresses the importance of the intrinsic solubility of the acid in determining its dissolution rate dependency on pH. The K_a of the acids also is important since it will determine, in combination with the intrinsic solubility, when deviation from Nernst behavior occurs with a change in bulk solution conditions.

With a further increase in the bulk solution pH, control of the dissolution rate also is affected by hydroxide ion diffusing in from the bulk solution, which reacts with the acid according to the equilibrium expression represented by Eq. 3. Thus, the total flux of the acid now includes the hydroxide-ion term, $D_{OH}([OH^-]_h - [OH^-]_0)$, because it numerically approaches the values of the other terms in the equation. A similar expression and interpretation was given by Higuchi *et al.* (5). The pH_0 rises at a rate that is directly dependent on the rate and amount of hydroxide ion diffusing in. Indomethacin, being poorly soluble, has little self-buffering capability and shows a sharp rise in its relative dissolution rate at a bulk pH of ~7.5. 2-Naphthoic acid is of intermediate solubility and shows a rise in its dissolution rate at a bulk pH of ~9.50 because the bulk hydroxide-ion concentration must be higher than that for indomethacin to overcome the greater self-buffering ability of 2-naphthoic acid at $X = 0$. Finally, at pH ~11.00, the considerable self-buffering capability of benzoic acid is overcome and an increase in the dissolution rate ensues with continued pH_{bulk} increase.

Further information can be derived from the profiles summarized in Fig. 7 if the terminal portion of the dissolution rate *versus* pH_{bulk} curve follows a limiting case of Eq. 22:

$$J = \text{constant} + \frac{D_{OH}}{h}([OH^-]_h - [OH^-]_0) \qquad \text{(Eq. 40)}$$

The $[H^+]_0 - [H^+]_h$ term in Eq. 22 is not actually constant since any change in $[OH^-]$ must give a corresponding change in $[H^+]$. However, at high bulk pH values, the hydrogen-ion term becomes negligible with respect to the hydroxide-ion term. A plot of *J versus* $[OH^-]_h - [OH^-]_0$ is shown in Fig. 9 for 2-naphthoic acid. In fact, $[OH^-]_0$ is negligible relative to $[OH^-]_h$ for all of the acids in this pH range, with a plot of *J versus* $[OH^-]_h$ having an essentially identical slope to that predicted from Eq. 40. Similar plots were made for benzoic acid and indomethacin, and the results are summarized in Table VIII.

The slopes of the three plots render values for the hydroxide-ion diffusivity that range from 2.63×10^{-5} to 3.04×10^{-5} cm^2/sec. A mean diffusivity of 2.79×10^{-5} cm^2/sec was determined, and this value was chosen for D_H and D_{OH} in the preceding theoretical calculations. Again, the assumption was made that the boundary layer thickness, *h*, used to calculate D_{OH} from the slopes in Table VIII is that calculated for the acid flux dependency on $\omega^{1/2}$. This assumption seems reasonable considering the good correlation between the experimental and calculated flux results and the consistency of the D_{OH} values. Nevertheless, it is an assumption open to question.

Apart from allowing an estimate of D_{OH} for this system, Eq. 40 also shows that at extremely high hydroxide-ion concentrations, the fluxes of all of the acids are identical and independent of the properties of the acid; *i.e.*, both the constant terms and $[OH^-]_0$ are negligible relative to the $[OH^-]_h$ term.

Concentration Profiles and pH across Diffusion Layer—Figure 10 shows idealized sections of the diffusion layer for benzoic acid, 2-naphthoic acid, and indomethacin at various bulk solution pH values. The fractional distance across the diffusion layer is calculated as X/h. Fractional concentrations are given by dividing the concentration of the species at $X = 0$ into that at $X = X$ in the case of HA, A^-, and H^+ or by dividing the concentration of the species at $X = h$ into that at $X = X$ for

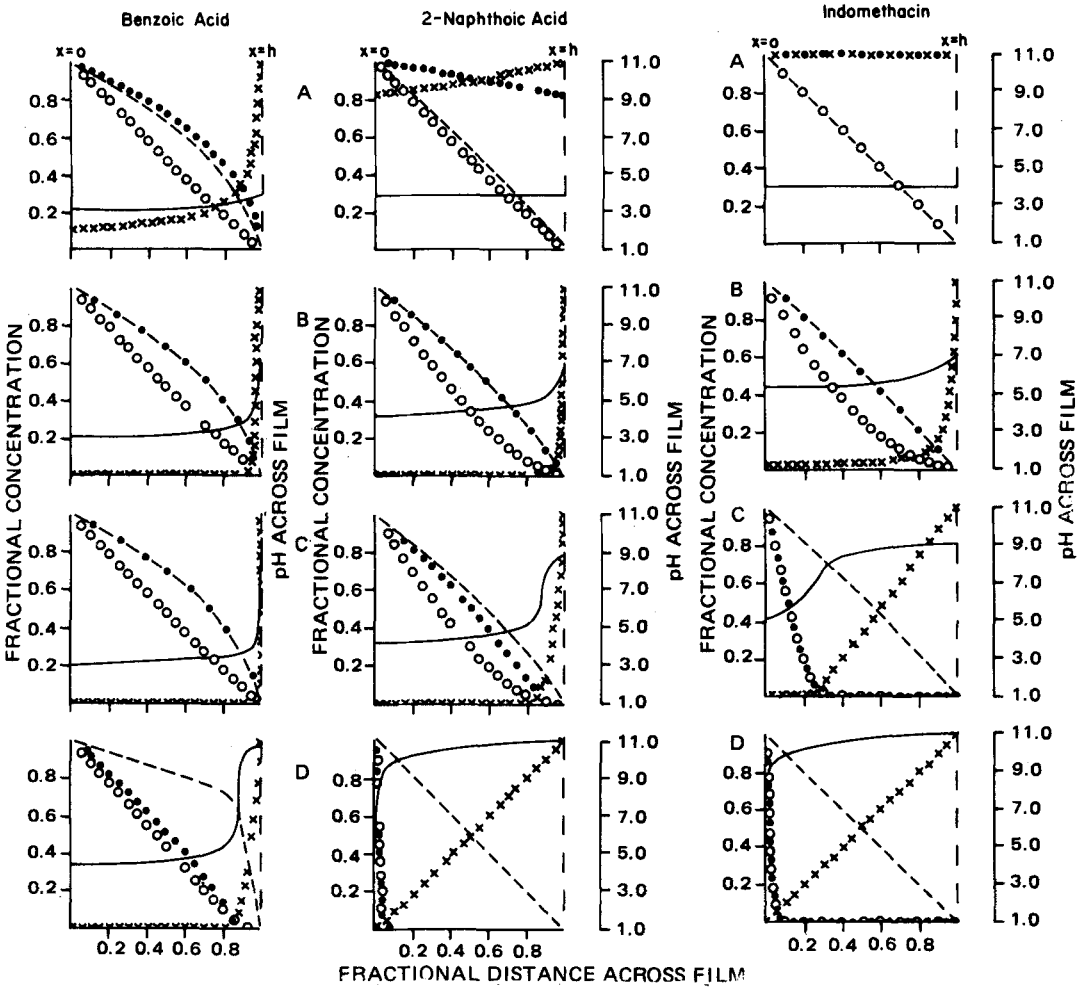

Figure 10—*Idealized diffusion layer cross sections for benzoic acid, 2-naphthoic acid, and indomethacin, showing the fractional concentration profiles with the fractional distance across the film as calculated from Eqs. 30 and 31. Calculated values of pH across the film in each case also are included. Key:* ○, *[HA];* – –, *[A⁻];* ●, *[H⁺];* ×, *[OH⁻];* —, *pH; A, pH_{bulk} 4.00; B, pH_{bulk} 7.00; C, pH_{bulk} 9.00; and D, pH_{bulk} 11.00.*

OH^-, which diffuses in the opposite direction to that of the other species. These functions normalize the data across the diffusion layer and facilitate comparison of concentration profiles for different compounds at the same bulk solution pH or for the same compound at different bulk solution pH. However, these values are useful only for comparative purposes and are obtained from the absolute data derived from Eq. 30 and its dependent equations.

The ability of benzoic acid to self-buffer the diffusion layer as $[H^+]_h$ varies is seen in Fig. 10 by observing the pH changes across the diffusion layer as a function of the bulk solution pH. Only at the rather high bulk solution pH of 11.00 does the hydroxide ion significantly affect pH_0 and, thus, increase the dissolution rate. 2-Naphthoic acid shows its ability to self-buffer between pH_{bulk} 4.0 and 9.00, after which the diffusion of hydroxide ion begins to affect the dissolution rate. Indomethacin, as discussed previously, is less able to effect its own pH microenvironment of the diffusion layer. In this case, the bulk solution pH largely determines pH_0 and, therefore, the dissolution rate of the drug under these conditions.

Table VIII—Hydroxide-Ion Diffusivity Calculated from the Slopes of the J_{obs} *versus* $[OH^-]_h - [OH^-]_0$ Plots for Benzoic Acid, 2-Naphthoic Acid, and Indomethacin

Compound	Slope[a] × 10^8	$h \times 10^3$ [b], cm	$D_{OH} \times 10^5$, cm^2/sec	r[c]
Benzoic acid	1.174	2.29	2.69	0.9964
2-Naphthoic acid	1.334	1.97	2.63	0.9987
Indomethacin	1.826	1.67	3.04	0.9898

[a] Units for $[OH^-]$ are moles per square centimeter. [b] Calculated from Eq. 31. [c] Correlation coefficient for each plot.

From the way in which the model has been developed, the diffusion layer thickness, h, from the Levich relationship has been taken as an absolute distance from the solid–liquid surface to where perfect mixing of the bulk solution abruptly occurs. This was shown by Levich (15), in electrochemical model systems, not to be totally correct. Rather, the concentration changes are more continuous around $X = h$. He showed that direct use of the postulated diffusion layer thickness in the Nernst relationship underestimates the true diffusion layer thickness and approximates the shape of the concentration profile. Gregory and Riddiford (39) also demonstrated that h is represented more correctly by a more complex expression than that used by Levich. However, the Levich–Nernst combination is a good approximation to the real situation, as supported by the agreement between the theory and the experimental data over wide ranges of bulk solution conditions in the present study.

CONCLUSIONS

The rotating-disk dissolution apparatus, combined with a potentiometric technique to maintain the bulk solution pH, has been demonstrated to be a convenient and precise system for the determination of dissolution rates of solid monoprotic acids into aqueous media. With minor modifications, the system is adaptable to the study of mass transport of basic compounds under similar conditions.

A theoretical approach has been presented to describe the factors that determine the dissolution rates of monoprotic acids into an unbuffered but constant pH aqueous solution where a simultaneous chemical reaction occurs with water and hydroxide ions of the bulk solution. The model adequately describes the initial dissolution rates of three carboxylic acids having a broad range of solubility properties under various pH conditions. The concept of a pH microenvironment within the diffusion layer is used

to explain the influence of several factors, such as the bulk solution pH, solubility, and diffusivity, on the dissolution rate of the acids.

REFERENCES

(1) W. Nernst, *Z. Phys. Chem.*, **47**, 55 (1904).

(2) E. Brunner, *ibid.*, **47**, 56 (1904).

(3) C. V. King and J. S. Brodie, *J. Am. Chem. Soc.*, **59**, 1375 (1937).

(4) A. W. Hixson and S. Baum, *J. Ind. Eng. Chem.*, **36**, 528 (1944).

(5) W. I. Higuchi, E. Parrott, D. Wurster, and T. Higuchi, *J. Am. Pharm. Assoc., Sci. Ed.*, **47**, 376 (1958).

(6) W. I. Higuchi, E. Nelson, and J. G. Wagner, *J. Pharm. Sci.*, **53**, 333 (1964).

(7) W. E. Hamlin and W. I. Higuchi, *ibid.*, **55**, 205 (1966).

(8) A. Fick, *Ann. Phys.*, **94**, 59 (1855).

(9) W. H. Steinburg, H. H. Hutchins, P. G. Pick, and J. S. Lazer, *J. Pharm. Sci.*, **54**, 625 (1965).

(10) *Ibid.*, **54**, 761 (1965).

(11) A. Shah, *J. Pharm. Sci.*, **60**, 1564 (1971).

(12) J. H. Collett, J. A. Rees, and N. A. Dickinson, *J. Pharm. Pharmacol.*, **24**, 724 (1972).

(13) F. Underwood and D. Cadwallader, *J. Pharm. Sci.*, **67**, 1163 (1978).

(14) J. H. Wood, J. E. Syrato, and H. Letterman, *ibid.*, **54**, 1068 (1965).

(15) V. G. Levich, "Physico-chemical Hydrodynamics," Prentice-Hall, Englewood Cliffs, N.J., 1962.

(16) S. Prakongpan, A. H. Molokhia, K. H. Kwan, and W. I. Higuchi, *J. Pharm. Sci.*, **65**, 685 (1976).

(17) A. Tsuji, E. Nakashima, S. Hamano, and T. Yamana, *ibid.*, **67**, 1059 (1978).

(18) A. Goldberg, in "Dissolution Technology," L. J. Leeson and J. T. Carstensen, Eds., Industrial Pharmaceutical Technology Section, APhA Academy of Pharmaceutical Science, Washington, D.C., 1974.

(19) M. Gibaldi, in "The Theory and Practice of Industrial Pharmacy," L. Lachman, H. Lieberman, and J. Kanig, Eds., Lea & Febiger, Philadelphia, Pa., 1970, p. 246.

(20) B. Carnahan, H. A. Luther, and J. O. Wilkes, "Applied Numerical Methods," Wiley, New York, N.Y., 1969, p. 171.

(21) D. D. Perrin, D. R. Perrin, and W. Armarego, "Purification of Laboratory Chemicals," Pergamon, Oxford, England, 1966.

(22) R. Pakula, L. Pichnej, S. Spychala, and K. Butkiewicz, *Pol. J. Pharmacol. Pharm.*, **29**, 151 (1977).

(23) S. Spychala, K. Butkiewicz, R. Pakula, and L. Picknej, *ibid.*, **29**, 157 (1977).

(24) "Physical Pharmacy," A. N. Martin, J. Swarbrick, and A. Cammarata, Eds., Lea & Febiger, Philadelphia, Pa., 1969.

(25) E. R. Garrett and C. H. Won, *J. Pharm. Sci.*, **60**, 1801 (1971).

(26) S. Goto, W. Tseng, M. Kai, S. Aizawa, and S. Iguchi, *Yakuzaigaku*, **29**, 118 (1969).

(27) B. R. Hajratwala and J. E. Dawson, *J. Pharm. Sci.*, **66**, 27 (1977).

(28) E. Pawetczyk and B. Knitter, *Pharmazie*, **33**, 586 (1978).

(29) H. Nogami, T. Nagai, and A. Suzuki, *Chem. Pharm. Bull.*, **14**, 329 (1966).

(30) A. H. Goldberg and W. I. Higuchi, *J. Pharm. Sci.*, **57**, 1583 (1968).

(31) G. L. Flynn, S. H. Yalkowsky, and T. J. Roseman, *ibid.*, **63**, 479 (1974).

(32) R. C. Reid and T. K. Sherwood, "Properties of Gases and Liquids," McGraw-Hill, New York, N.Y., 1966.

(33) "International Critical Tables of Numerical Data, Physics, Chemistry and Technology," McGraw-Hill, New York, N.Y., 1926.

(34) S. Dayal, T. Higuchi, and I. Pitman, *J. Pharm. Sci.*, **61**, 695 (1972).

(35) R. H. Stokes, *J. Am. Chem. Soc.*, **72**, 2243 (1950).

(36) S. B. Tuwiner, "Diffusion and Membrane Technology," Reinhold, New York, N.Y., 1962, p. 378.

(37) T. Erdey-Grûz, "Transport Phenomena in Aqueous Solutions," Wiley, New York, N.Y., 1974.

(38) D. Eisenberg and W. Kauzman, "Structure and Properties of Water," Oxford University Press, New York, N.Y., 1969, pp. 217–224.

(39) D. P. Gregory and A. C. Riddiford, *J. Chem. Soc.*, **1956**, 3756.

ACKNOWLEDGMENTS

Adapted in part from a dissertation submitted by K. G. Mooney to the University of Kansas in partial fulfillment of the Doctor of Philosophy degree requirements.

Supported by Grant GM22357 from the National Institutes of Health.

Dissolution Kinetics of Carboxylic Acids II: Effect of Buffers

K. G. MOONEY *, M. A. MINTUN ‡, K. J. HIMMELSTEIN, and V. J. STELLA ˣ

Received March 24, 1980, from the *Departments of Pharmaceutical Chemistry and Chemical and Petroleum Engineering, University of Kansas, Lawrence, KS 66045.* Accepted for publication July 3, 1980.

*Present address: Boehringer Ingelheim, Ridgefield, CT 06877. ‡Present address: Washington University, St. Louis, MO 63110.

Abstract □ The dissolution behavior of 2-naphthoic acid from rotating compressed disks into aqueous buffered solutions of constant ionic strength (μ = 0.5 with potassium chloride) at 25° was investigated. A model was developed for the flux of a solid monoprotic carboxylic acid in aqueous buffered solutions as a function of the solution pH and the physicochemical properties of the buffer. The model assumes a diffusion layer-controlled mass transport process and a simple, instantaneously established reaction equilibrium between all reactive species (acids and bases) across the diffusion layer. Using intrinsic solubilities, pKa values, and diffusion coefficients, the model accurately predicts the dissolution of 2-naphthoic acid as a function of the bulk solution composition. The concentration profiles of all species across the diffusion layer are generated for each buffer concentration and bulk solution pH, including the pH profile within the microclimate of the diffusion layer and the pH at the solid–solution boundary.

Keyphrases □ Carboxylic acids—dissolution kinetics, effect of buffers □ Dissolution kinetics—carboxylic acids, effect of buffers □ Buffers—effect on dissolution kinetics of carboxylic acids

The objective of this investigation was to determine experimentally the effect of buffers on the dissolution of 2-naphthoic acid from a constant surface area pellet under controlled ionic strength (μ = 0.5 with potassium chloride), temperature (25°), and pH conditions (pH-stat). A model, an extension of one described previously (1), also was de-

0022-3549/81/0100-0022$01.00/0